Article

Superlative and Selective Sensing of Serotonin in Undiluted Human Serum Using Novel Polystyrene Sulfonate Conductive Polymer

Victoria E. Coyle, Michael C. Brothers, Sarah McDonald, and Steve S. Kim*

Read Online

ACCESS | Metrics & More | Article Recommendations | SI Supporting Information

ABSTRACT: In the past 5 years, real-time health monitoring has become ubiquitous with the development of watches and rings that can measure and report on the physiological state. As an extension, real-time biomarker sensors, such as the continuous glucose monitor, are becoming popular for both health and performance monitoring. However, few real-time sensors for biomarkers have been made commercially available; this is primarily due to problems with cost, stability, sensitivity, selectivity, and reproducibility of biosensors. Therefore, simple, robust sensors are needed to expand the number of analytes that can be detected in emerging and existing wearable platforms. To address this need, we present a simple but novel sensing material. In short, we have modified the already popular PEDOT/PSS conductive polymer by completely removing the PEDOT component and thus have fabricated a polystyrene sulfonate (PSS) sensor electrodeposited on a glassy carbon (GC) base (GC-PSS). We demonstrate that coupling the GC-PSS sensor with differential pulse voltammetry creates a sensor capable of the selective and sensitive detection of serotonin. Notably, the GC-PSS sensor has a sensitivity of 179 μA μM^{-1} cm^{-2} which is 36x that of unmodified GC and an interferent-free detection limit of 10 nM, which is below the concentrations typically found in saliva, urine, and plasma. Notably, the redox potential of serotonin interfacing with the GC-PSS sensor is at −0.188 V versus Ag/AgCl, which is significantly distanced from peaks produced by common interferants found in biofluids, including serum. Therefore, this paper reports a novel, simple sensor and polymeric interface that is compatible with emerging wearable sensor platforms.
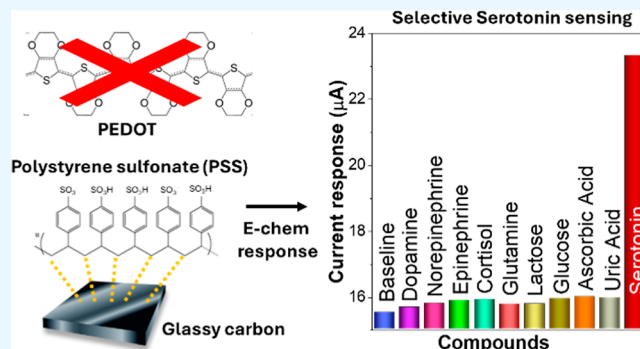
1. INTRODUCTION

Advances in electronics and sensor technologies have enabled wearables equipped with real-time sensors that measure the concentration of biochemicals to report on the physiological state.[1−3] However, despite the ubiquitous nature of continuous glucose monitors, few other real-time sensors are commercially available. One common class of compounds currently being explored for real-time sensor applications is monoamine neurotransmitters. Monoamine neurotransmitters, including catecholamines (dopamine, adrenaline and noradrenaline) as well as serotonin are known to correspond to and be key indicators of both fatigue and general mental wellbeing.[4,5]

Sensor researchers have focused on the detection of monoamine neurotransmitters, including catecholamines and serotonin, as they are inherently redox-active. As a result, these analytes can be detected directly due to isolated changes in current response at specific voltages correlating to analyte concentration. This contrasts with other sensor methods that rely on enzyme-mediated reactions,[6,7] the presence of exogenous redox reporters[8] to produce the electrochemical signal, or other more complicated schemes.[5,9−12]

Part of the challenge in deploying real-time neurotransmitter sensors is that most monoamine neurotransmitters are found

in trace concentrations of biofluids (<1 nM). However, serotonin is present at appreciable concentrations in many biofluids (>100 nM), and thus is a promising analyte for real-time detection. Serotonin or 5-hydroxytriptamine (5-HT) is a neurotransmitter of particular interest, as it is a key contributor toward sleep, mood, and appetite regulation.[13] Serotonin has a redox-active indole functional group as opposed to a catechol functional group, and, as a result, should have different electrochemical properties compared to other monoamine neurotransmitters. Serotonin concentrations are most readily measured (due to their highest concentrations) in urine (0.3−1.6 μM)[14] and blood (0.27−1.5 μM).[15] Serotonin has been found within cerebral spinal fluid (<0.057 nM)[16] but at concentrations significantly lower than in other biofluids. Even in the best of circumstances, these concentrations are
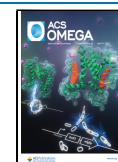
significantly lower than lactate and glucose levels (∼mM) which are the only successful electrochemical sensors for bioanalytes.[17,18] A deployable serotonin sensor must not only be sensitive enough to detect these micromolar to nanomolar ranges, but also retain significant selectivity against analytes that are present in concentrations substantially higher (>1000×) than serotonin.

To overcome this challenge, voltammetric methods are often used that can identify redox-active compounds based on their redox potential. However, voltammograms of biological fluids are complex, as redox active analytes are inherent in biofluids, including NADH,[19] FADH$_2$, catecholamines (e.g., dopamine, norepinephrine, epinephrine),[20] uric acid,[21] ascorbic acid,[22] and tyrosines.[23] As a result, the voltammograms can have overlapping peaks, thus confounding analysis; many of these potential interfering agents are at concentrations equal to or greater than serotonin. Sensor and method design must account for these complications. Notably, to selectively detect serotonin, the method must be able to discriminate among catecholamines (e.g., dopamine, norepinephrine, and epinephrine), redox-active metabolites (e.g., uric acid), and indoles (e.g., serotonin).

While bare carbon or metallized electrodes[24−27] can detect serotonin and other monoamine neurotransmitters, the application of a matrix on top of the electrode typically helps with sensitivity and selectivity through increasing surface area and/or adding functional groups with improved binding energies. Conductive polymers have been repeatedly demonstrated to improve the sensitivity and lower the limit of detection compared to that of simple gold or carbon electrodes. Currently common conductive and copolymers that have shown much promise in the field of neurotransmitter sensors are poly(3,4-ethylenedioxycythiophene)/polystyrene sulfonate (PEDOT/PSS),[28,29] polypyrrole (PPy),[30−32] and nafion.[33−35] Conductive polymers, especially those that are composed of ionic matrices, have high electrical conductivity and thus do not passivate electrodes. However, because of their thickness, conductive polymers have broader peaks due to diffusion into the polymeric matrix and/or voltage drops across the conductive polymer.[36] The result is that conductive polymers can suffer from peak broadening, thus, reducing resolution and adding another complication to neurotransmitter identification and quantitation. Some conductive polymers have poor conductance, resulting in high overpotentials that again frustrate measurements.[37] An optimized conductive polymer coating is needed that (1) can effectively enrich monoamine neurotransmitters, (2) has high conductance (a low overpotential), and (3) can operate as a thin-film and thus minimize the impact of Warburg diffusion on the voltammogram.

In the literature, graphene and graphene oxide sensors, along with nafion and PEDOT/PSS sensors, have demonstrated the greatest promise with regards to selectivity and sensitivity. The commonality in these sensors is aromaticity (graphene, graphene oxide, polystyrene sulfonate) and a high density of negative charges (nafion, PSS, graphene oxide). These functional groups should have improved binding energies and thus higher affinity to monoamine neurotransmitters due to electrostatic and π−π stacking interactions. PSS has both an aromatic group and a negatively charged sulfonate in each monomeric unit and thus contains both a high density of aromatic groups and negative charges. Therefore, PSS has the

potential to enhance neurotransmitter affinity, resulting in an improved sensitivity and limits of detection (LOD).

In this paper, we propose and demonstrate a sensor that modifies the PEDOT/PSS framework where PEDOT, the positively charged copolymer, has been removed from the system and PSS has been electrodeposited on its own. To the authors' knowledge, this paper presents the first of its kind to electrodeposit a specific PSS matrix without a copolymer and use it as a sensing material. The resulting Glassy carbon (GC)—PSS sensor resulted in a superior sensor response. Notably, we demonstrate that this matrix causes a significant shift in the redox potential of serotonin, indicating a change in its electrostatic state, significantly removing the peak from common interferences including uric acid and catecholamines that frustrate selectivity and sensitivity in many neurotransmitter sensors in the literature. The sensor, while having reduced sensitivity in serum, still can detect serotonin at physiological concentrations. Therefore, this article provides a simple, unique sensor for real-time detection and monitoring of serotonin in biofluids.

2. METHODS

2.1. Chemicals. All chemicals were procured from Sigma-Aldrich and used as received, apart from the human serum. Human serum samples were purchased from Sigma-Aldrich and are human male plasma (type AB) sterile-filtered hemoglobin. Diluted human serum was done using 1× phosphate-buffered saline (PBS) for 25, 50 and 75% serum volumes. 100% serum was used as delivered.

2.2. Electrochemical Set-Up. All electrochemistry experiments were performed with a CH Instrument (CHI660E) potentiostat. A 3-electrode setup was used for all experiments. Working electrodes were R2 mm GC discs (CH Instruments). Reference electrodes were Ag/AgCl (+0.197 V vs SHE) (CH Instruments). Counter electrodes were platinum-coated titanium rods (EDAQ Inc.).

2.3. Fabrication of GC-PSS and GC-PEDOT/PSS Electrodes. GC electrodes were polished using an electrode polishing kit per manufacturer's instructions (CH Instruments). Electrodeposition onto the GC working electrode was performed at +2 V vs Ag/AgCl in a fresh solution of 0.4% poly(sodium 4-styrenesulfonate) in Milli-Q water for PSS deposition and a combination solution of 0.4% Poly(sodium 4-styrenesulfonate) and 0.3% 3,4-ethylenedioxythiophene in Milli-Q water for PEDOT/PSS deposition. After electrodeposition, sensors were rinsed with Milli-Q water and air-dried. All sensor surface areas were kept consistent with Kapton tape using a diameter (ø) of 4 mm were calculated to have a geometric active surface area of 0.126 cm^{-2}.

2.4. Characterization of GC-PSS Sensor. Scanning electron microscopy (SEM) was used to determine the surface morphology and the effectiveness of electrodeposition of the conductive polymer. SEM was performed by using a Zeiss GeminiSEM 500 instrument. Electrochemical surface area (ECSA) characterization was performed in 1 M H$_2$SO$_4$ solution at a sweep rate of 100 mV s^{-1}.

2.5. Sensing of Serotonin Using GC-PSS Electrodes. Differential pulse voltammetry (DPV) was performed by using the following parameters: Scan range of −0.7 to +0.7 V; AC amplitude of 50 mV; pulse width of 0.5 s; sampling width of 0.0167 s; and pulse period of 0.5 s. Sensors were equilibrated by running through at least five scans before performing electrochemical measurements for either serotonin or con-
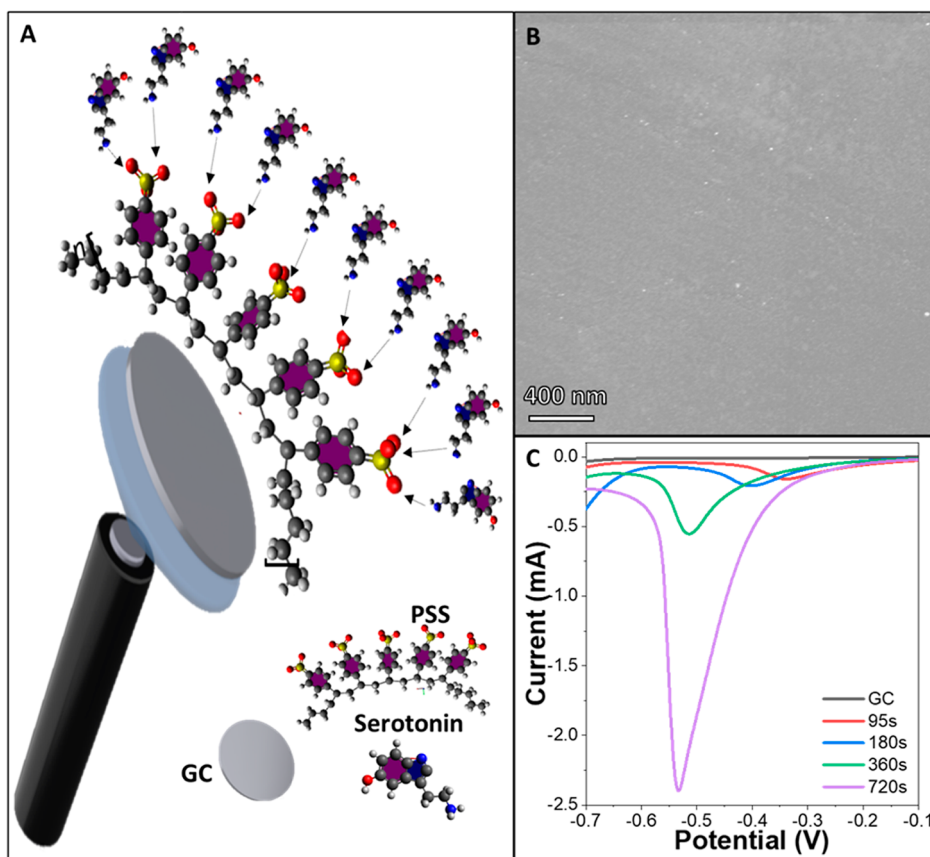
Figure 1. (A) Schematic of fabricated sensor of GC rod electrode with attachment of PSS and serotonin interacting with the surface of PSS (B) SEM image of GC-PSS sensor. (C) ECSA of GC-PSS sensor for various electrodeposition times (0,95,180, 360, and 720 s).

taminants in buffer (1× PBS), serum, or serum diluted in PBS. A dwell time of 7 min was implemented to allow for serotonin penetration of the polymer matrix after each addition before DPV measurements were performed. Peak current height, calculated as the difference in current between −0.6 V and the maximum current around −0.2 V, was reported for sensor response and sensitivity calculations.

3. RESULTS AND DISCUSSION

3.1. GC-PSS from the GC-PEDOT/PSS Concept.
Serotonin can be detected directly using metallized and carbon-based electrodes.[24−26] To improve the sensitivity of these electrode materials, recognition elements, including polymers and biopolymers, have been explored. Notably, conductive polymers have commonly been used in the literature for electrochemical neurotransmitter sensors. This initially led us to investigate the commonly used material PEDOT/PSS as a starting material for our studies; PEDOT/PSS has been successfully implemented into electrochemical sensors for a large range of analytes. Therefore, as a baseline, we analyzed the performance of PEDOT/PSS for detecting serotonin using DPV.

PEDOT/PSS was electrodeposited onto GC electrodes (see Methods section). The electrodes were then interrogated using DPV in the presence of increasing concentrations of serotonin. The GC-PEDOT/PSS sensor was able to detect concentrations as low as 200 nM at a potential of −0.188 V (Figure S1). In comparison, no response was observed for GC alone at the same potential (Figure S2). GC did have a unique interaction (as observed by the presence of a peak) with

serotonin at + 0.32 V for concentrations of serotonin greater than 200 nM. However, neither GC alone nor GC-PEDOT/PSS could detect at low enough concentrations to detect the full range of serotonin found in biofluids (urine, blood, and saliva) despite their prevalence in the literature.

Previous literature shows that the presence of negatively charged functional groups, such as carboxylates present in graphene oxide and sulfonates in nafion and PSS, is common among reported conductive polymers for sensing serotonin. All of these negatively charged materials are likely to enrich serotonin via charge−charge attraction with monoamine present in serotonin. Additionally, aromatics found in graphene, graphene oxide, and PSS were also common among conductive polymers for detection of serotonin; this would putatively support π−π stacking interactions and thus have favorable binding energies for indole rings. Therefore, PSS having the highest concentration of both negatively charged and aromatic groups was further explored as a unique polymeric recognition element.

3.2. GC-PSS Sensor Characterization.
Figure 1A shows the GC-PSS preparation scheme where a GC rod electrode was used as the working electrode and a PSS coating was electrodeposited onto the surface where serotonin is attracted to the free SO_3^- side chains. Unlike other methods of conductive polymer electrodeposition our technique involved no wait times for sample preparation,[38] a singular component (polystyrene sulfonate) unlike other conductive polymer procedures[39] and a single-step rapid preparation method. To further understand the surface morphology of the electrodeposited PSS, SEM analysis was performed as shown in
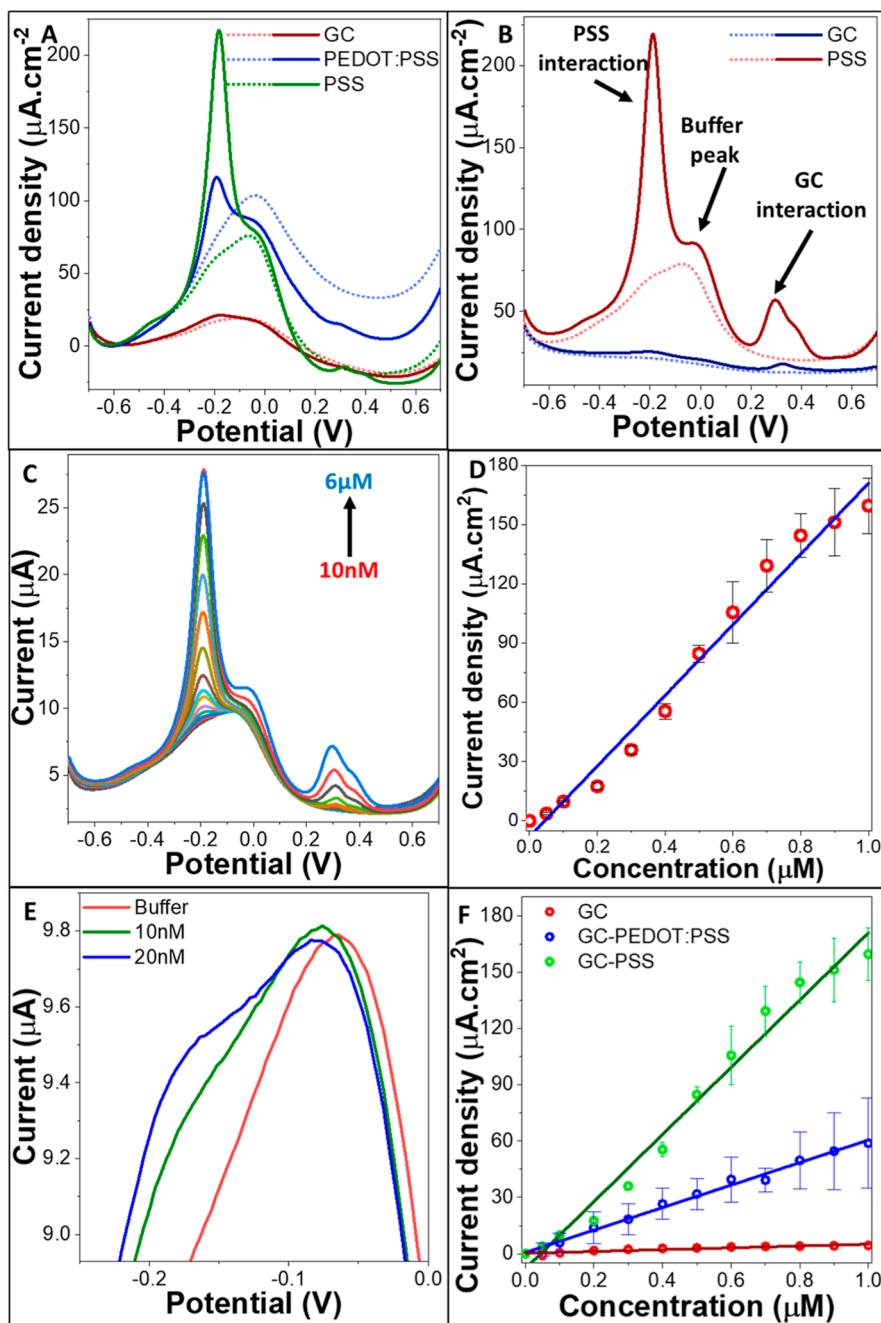
Figure 2. (A) DPV curves comparing unmodified GC sensor (red), GC-PEDOT/PSS sensor (blue), and GC-PSS sensor (green) in 0.1 M PBS (pH = 7.4) buffer (dotted lines) and 1 μM Serotonin (solid lines) (B) DPV curves of GC (blue) and modified GC-PSS (red) electrodes comparing PBS buffer (dotted lines) response and 6 μM Serotonin (solid lines) to identify redox peaks (C) DPV analysis of GC-PSS sensor with increasing concentrations of serotonin (10 nM–6 μM) in 0.1 M PBS (pH = 7.4), (D) the calibration curve of the GC-PSS within the concentration range of 0–1 μM serotonin, (E) DPV curves of the GC-PSS sensor showing real detection limit. (F) DPV peak current responses of serotonin between 0 and 1 μM for GC (red), GC-PEDOT/PSS (blue), and GC-PSS (green). (All error bars of st. dev. for $n = 3$).

Figure 1B. The high magnification image of the deposited PSS (Figure S3A) shows a texturized surface and thus the presence of the electrodeposited conductive polymer. Although textured, the surface maintains a smoothness similar to that of the deposited GC-PEDOT/PSS (Figure S3C,D) and the unmodified GC (Figure S3E,F). The minimal change in surface morphology suggests that changes in the functional groups present within the conductive polymer, and not changes in morphology, are responsible for the enhanced sensing capabilities of the GC-PSS sensor.

ECSA measurements (Figure 1C) performed by cyclic voltammetry in H_2SO_4 were used to determine the surface area based on the reduction peak area. The peak area was converted to electrode surface area using the reported Carbon monoxide stripping charge parameter of 420 μC.cm^{-2}[40] using the formula outlined by Coyle et al.[41] The real surface areas of 0, 95, 180, 360, and 720 s GC-PSS sensors were calculated to be 0.18, 1.37, 2.11, 3.21, and 10.6 cm^2 respectively. An interesting phenomenon was observed with increasing deposition time as peak position shifted more negative. This can be explained via more PSS deposition onto the surface. As the SO_3^- is reacting

Scheme 1. Proposed Mechanism of GC-PSS Interaction with Serotonin
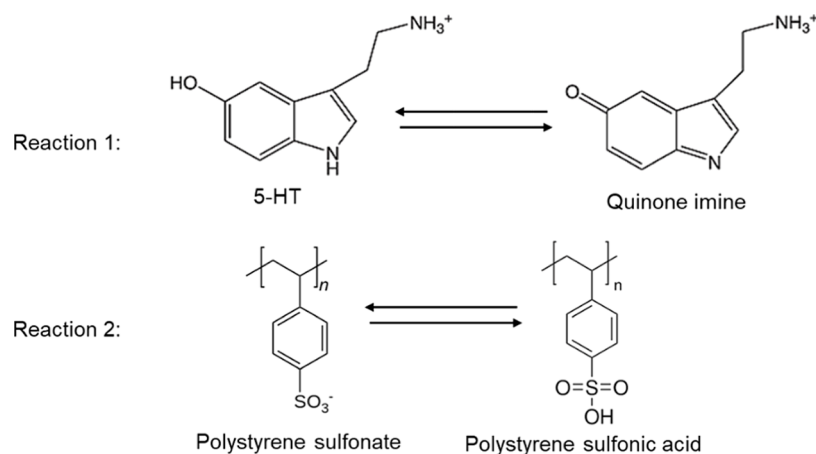
with the H^+ the less amount of SO_3^- on the surface causes a more rapid depletion off the electrode surface. The peaks appear to all start at the same potential (-0.1 V) however, all deplete at different potentials until you reach 360 s where it reaches its equilibrium point (-0.53 V).

To ensure this newly developed sensor was in fact improved upon compared to its PEDOT/PSS predecessor, we performed a DPV analysis as can be seen in Figure 2A. The DPV curves (after baseline correction) represent an unmodified GC, a GC-PEDOT/PSS, a GC-PSS, and a GC-PSS electrode in a solution of 1 μM Serotonin. The current response (peak height) enhancement of the GC-PSS with a rapid electrodeposition time of 95 s compared to the GC and GC-PEDOT/PSS is 15.2× and 9×, respectively, which is a significant enhancement considering the slight modification made to the starting materials. This supports that the PSS in PEDOT/PSS is key to improving sensor performance with neurotransmitters.

3.3. Electrochemical Sensing of GC-PSS in PBS Solutions. The GC-PSS electrodes and their interaction with serotonin were studied via DPV as shown in Figure 2B. Initially the sensor was equilibrated by running at least five voltammograms in PBS solution until a stable voltammogram was achieved (current change of <0.1% for all applied voltages). For preliminary studies, 6 μM of serotonin was then injected and allowed to stabilize for 30 min to allow full binding/equilibration. The sensor was then interrogated using DPV. The resulting voltammogram had two new peaks, one at -0.188 V (previously unreported) and one at $+0.36$ V (more commonly reported). To verify that the interaction of serotonin with PSS was resulting in the peak at -0.188 V, a plain GC electrode was run side-by-side. The resulting scan lacked the peak at -0.188 V, and only had a new peak emerge at $+0.36$ V. Comparing the two scans it is likely that the peak forming at $+0.36$ V is appearing due to the interaction of GC and serotonin. While the amount of GC present for each electrode is equivalent, the presence of the PSS on the electrode surface for the GC-PSS electrode has clearly enhanced the current response of the GC-serotonin peak at $+0.36$ V. Additionally, a second peak now forms at -0.188 V; this peak only appears when both PSS and serotonin are present, indicating that a PSS–serotonin complex is forming. Notably, this change in peak position is not observed with any other serotonin sensor, including PEDOT/PSS, Nafion, or graphene oxide serotonin sensors. We hypothesize that this unique peak may be due to the PSS donating electrons to the

serotonin and thus stabilizing the oxidized state of serotonin. With the above-mentioned hypothesis, we would expect to observe a separate serotonin oxidation peak at the inherent, unmodified redox potential of serotonin ($\sim+0.36$ V), where lower concentrations result in a peak only at -0.188 V and higher concentrations result in a peak both for serotonin bound to PSS (as observed by a peak at -0.188 V) as well as free serotonin (as observed by a peak at $+0.36$ V). Due to these findings, we have deduced the resultant mechanism (Scheme 1) between our GC-PSS sensor consists of a reversible oxidation of serotonin converting the aromatic hydroxyl functional group to a ketone.[42] Protons formed during serotonin oxidation are likely to protonate the sulfonate and change the acidity at the surface of the conductive polymer and thus electrochemical properties.[43]

The voltammograms as a function of the serotonin concentration for GC-PSS sensors were then acquired. The sensor was exposed to increasing concentrations of serotonin starting at 10 nM and terminating at 6 μM using the same DPV parameters (Figure 2C). The peak at -0.188 V showed a steady rise in current response with increasing concentrations of serotonin where the peak at $+0.36$ V increased as a function of concentration but only appeared at micromolar concentrations. In comparison, the GC showed minimal current change at -0.188 V in the presence as a function of serotonin concentration with a small peak forming at $+0.36$ V at higher concentrations of serotonin. This is consistent with serotonin complexed with GC-PSS having a redox potential at -0.188 V.

3.4. Effect of GC-PSS-Coating Formulation on Serotonin Sensing. To determine the optimal GC-PSS sensor for performance in serotonin, each modified sensor grown at various times (95, 180, 360 and 720 s) were interrogated using DPV. Voltammograms were obtained first for the sensor in PBS buffer solution and then after an injection of 6 μM serotonin and then analyzed as can be seen in Figure S4. Absolute peak height as well as% increase in peak height at -0.188 V versus buffer was reported (Figure S5) to compare sensor sensitivity toward serotonin. The raw curves of each sensor where the 95 and 180 s sensors can be seen to show a dramatically sharp peak at -0.188 V compared to the buffer peak. However, higher deposition times (360 and 720 s) display higher raw current responses ($\sim$96 μA) in serotonin compared to the buffer peak show less of an affinity toward serotonin adsorption onto the sensor surface due to minimal current change versus the buffer peak height. This is further

Table 1. Comparison Table of PEDOT-Based Electrochemical Sensors for Serotonin Detection

sensor	technique	peak potential	linear range (μM)	detection limit (nM)	refs
rGO-PEDOT/PSS	amperometry/DPV	+0.4 V vs Ag/AgCl	-	100	28
GCE-PEDOT-RGO-Ag nanocomposite	amperometry/DPV	+0.28 V vs Ag/AgCl	0.1−500	100	44
NiO/CNT/PEDOT	DPV	+0.33 V vs SCE	0.3−20	63	45
AN-PEDOT/CNTs	amperometry/DPV	+0.4 V vs Ag/AgCl	1−100	50	46
FTO-PEDOT: PSS/ 3IP-TPyP	CV/EIS		1.7−138	230	29
PEDOT/Pt	CV/LSV	+0.4 V vs Ag/AgCl	20−100	71	47
GC-PSS	**DPV**	**−0.188 V vs Ag/AgCl**	**0.01−1**	**10**	**this work**
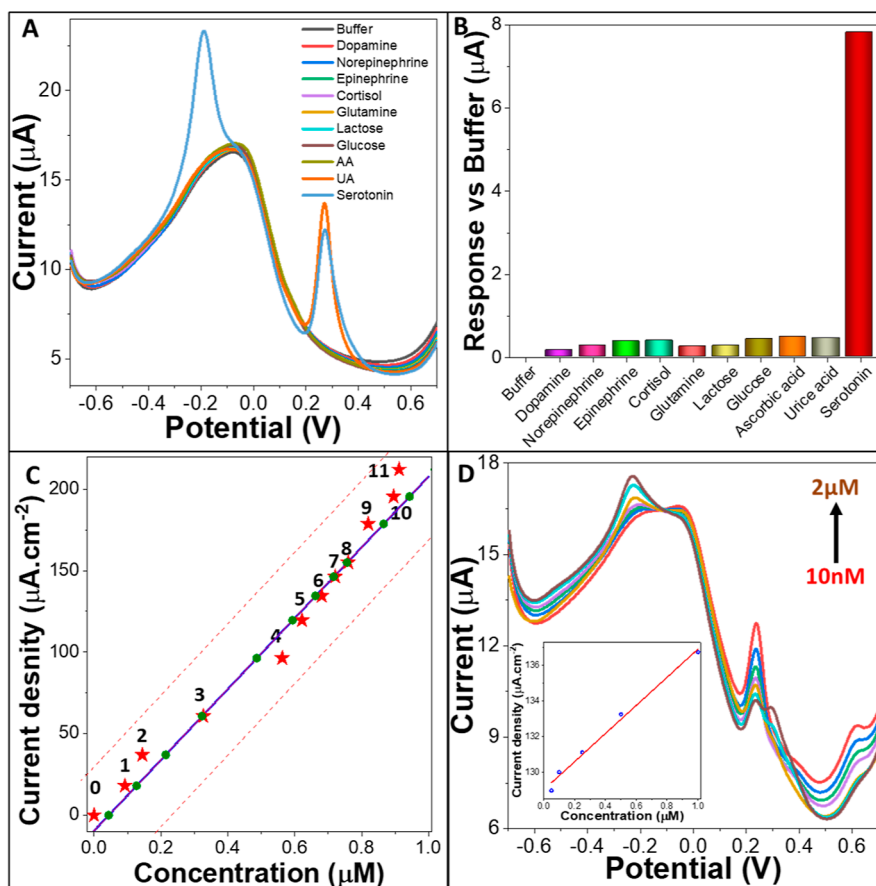
Figure 3. (A) DPV scans of the GC-PSS sensor in the presence of physiological contaminants with each contaminant injected into the system (B) a bar-graph representation of peak height response of the GC-PSS sensor and physiological contaminant interaction at −0.188 V (C) Unknowns analysis of GC-PSS in 0.1 M PBS (pH = 7.4) with added concentrations of serotonin with the concentration range of 10 nM and 1 μM (red dash lines represent the range of variability for each addition and numbers represent a serotonin concentration highlighted in Table S2) and (D) DPV curve of the GC-PSS sensor in 100% human serum with serotonin concentrations injected into the solution within a range of 10 nM−2 μM. Inset image of calibration curve of peak current response at −0.224 V.

examined where current change versus the buffer is displayed. The 95 s sensor outperforms all other sensors in the presence of serotonin showing a 140% change in current compared to the buffer in 6 μM serotonin while the 180 s deposition having a marginally lower percent increase in peak height (120%). Although the 360 and 720 s sensors clearly had much larger overall (magnitude) current responses their normalized (% current change) compared to the buffer were like that of an unmodified GC sensor varying only by 20%; we hypothesize that this is because the PSS acts as an ion conducting matrix, and thus promotes background water and proton oxidation. As a result of this analysis the 95 and 180 s PSS deposition GC-PSS sensors were chosen to further provide the sensitivity as calculated by the % change in current for 6 μM serotonin.

Thinner coatings were not explored, as the potential gain in sensitivity from this study appeared to be marginal.

3.5. Sensitivity, Linear Range, and LOD. Peak height and peak area are both data outputs that are typically linked to the analyte concentration for voltammogram measurements. As described in the methods, this manuscript uses peak height due to the simplicity of its calculation and the fact that it is less sensitive to changes in its baseline. The sensitivity of the sensor was determined using the peak height of the DPV results at −0.188 V compared to baseline from the serotonin titration experiments taken from Figure 2C. The resulting plot of peak height versus concentration is reported on Figure 2D.

The titration curve demonstrated that the sensor has a linear range between the concentrations of 10 nM and 1 μM (full peak height range calibration curve shown in Figure S6); this is

supported by an R^2 value of 0.98. The sensitivity, derived from the slope, was calculated as 178.99 μA μM^{-1} cm^{-2} and a detection limit of 10 nM visualized by Figure 2E; this change in current at −0.188 V as a function of serotonin was confirmed by the subsequent addition of 20 nM serotonin. In comparison, the unmodified GC electrode had an overall sensitivity of 4.9 μA μM^{-1} cm^{-2} and an R^2 of 0.859 over the entire titration curve with a detection limit of 200 nM. The bare GC electrode had two separate linear ranges, the first observed between 0 and 100 nM and the second observed between 100 nM and 1 μM (Figure S7). Notably, when comparing the GC electrode to the GC-PSS electrode, the GC-PSS demonstrated an enhancement of sensitivity of 36× compared to the flat GC electrode as well as an improved linear range.

To validate that the conductive polymer alone was not responsible for the improved performance, a titration curve from a GC-PEDOT/PSS was analyzed. The sensitivity calculated from the titration curve (Figure S8) was 59.9 μA μM^{-1} cm^{-2} with reasonable linearity over the titration range (R^2 value of 0.925). While some sensitivity was regained over GC alone, the sensitivity remained 3× lower than the reported GC-PSS electrode. Additionally, the linearity is poor across all concentrations. The detection limit for the GC-PEDOT/PSS was observed at 200 nM. To further validate the superiority of the GC-PSS sensor compared to the unmodified GC and the GC-PEDOT/PSS calibration curves have been placed along the same axis in Figure 2F for a visualized comparison.

Thus, the GC-PSS sensor has both a larger linear range than GC and GC-PEDOT/PSS, as well as greater sensitivity, improving the confidence of measurements and reducing the impact of noise, especially in complex biological samples. A comparison to other literature sensors is provided in Table 1.

3.6. GC-PSS Serotonin Sensor—Impact of Interfering Agents.
To test the robustness and selectivity of our sensor, we introduced common small biological molecules including redox-active species. All interfering species were added at or above the high end of physiological concentrations to validate that the sensor could work even in the worst-case conditions; concentrations of interferences tested are listed in Table S1. We then performed the same DPV measurements used for the detection of serotonin to identify any changes in the baseline and/or new peaks indicative of redox-active interferents (Figure 3A). The interference assay curve was organized as follows. First, the neurotransmitters that are commonly measured in addition to serotonin were added to the sensor including the catecholamines (dopamine, norepinephrine, and epinephrine) as well as the stress hormone cortisol. Addition of these interferences showed no response and no new peaks forming in the DPV curve. Then, the amino acid glutamine and the sugars lactose and glucose were added; while the sugars and amino acids groups do not have reversible redox active functional groups, they are at high concentrations and could still interfere via irreversible oxidation. As expected, no change in the peak height at −0.188 V was observed as a function of adding in these metabolites/sugars. To this mixture, the redox active metabolite ascorbic acid was then added and interrogated using DPV. The result was no response. Finally, another redox active metabolite, uric acid was added. A new peak was observed in DPV analysis. However, the peak position (+0.25 V) is sufficiently distanced from the serotonin peak to enable clear resolution. Additionally, the peak stabilized almost instantly and did not change

after a three-minute stabilization period, indicating that the PSS matrix was not concentrating uric acid to the electrode surface.

Overall, no appreciable changes in the peak at −0.188 V were observed (Figure 3B) upon the addition of interferences. Serotonin was then introduced to validate that the sensor could still detect the primary target even in the presence of interfering agents, resulting in a current change of 7.82 μA after spiking the solution with 1.2 μM of serotonin. This value was lower than originally obtained in pure buffer (13.89 μA) as the complex media unsurprisingly hinders the sensors response. However, this can likely be accounted for in complex media. More importantly, the data strongly suggest that none of the potential interfering biochemicals would result in peaks directly overlapping with the serotonin redox peak and thus provide false positive results or confounding results.

3.7. Validation of GC-PSS Sensor Calibration Curve.
To determine the ability of the GC-PSS sensor to predict concentration as a function of response, increasing concentrations of serotonin were titrated onto the sensor surface; the serotonin concentrations added to the sensor differed from the standard curve. Specifically, serotonin concentrations within the sensing range of 10 nM and 1 μM were added to the sensor, measured, and reported (Figure 3C).

The calibration curve from the sensitivity analysis (Section 3.5) was used to predict serotonin concentration from peak height. The equation is as follows: $y = 178.99x − 7.97$. Table S2 shows the actual and calculated concentrations for each measurement. As expected, while some variance between actual and calculated concentrations was observed, the discrepancies were minor. The average response change (%) between the real and calculated concentrations was under 10%. Notably, concentrations between 300 nM and 1 μM showed a variance between calculated and actual serotonin concentration of ∼ 5%; this is expected, as the greater peak height reduces systemic error. Thus, the GC-PSS sensor can be used to measure and quantify the unknown concentration of serotonin in samples.

3.8. GC-PSS-Sensing Studies in 100% Human Serum.
To analyze the sensors capabilities in biological fluids, the sensor was tested in various serum samples both in the presence and absence of exogenous serotonin. Figure 3D shows the DPV response curves of the GC-PSS sensor in 100% serum with increasing concentrations of titrated serotonin (10 nM−2 μM). The serotonin peak has been slightly shifted to the negative with the peak current potential now appearing at −0.224 V (a shift of −0.036 V).

Further examining Figure 3D, three key areas of the DPV voltammogram can be identified correlating to the addition of serotonin; a peak corresponding to the serotonin interaction with GC-PSS (peak at −0.224 V), a large peak at + 0.3 V which from the interference studies we assume is from uric acid or other serum interferants, and a slight peak at + 0.65 V which is not due to any of the contaminants examined. Notably, the observed peaks at + 0.3 and +0.65 V decrease as a function of scan number and thus appear to be inherent to redox active species in the serum. Fortunately, neither of those peaks overlaps with the serotonin peak at −0.224 V.

To analyze the effectiveness of the GC-PSS in serum, we used the peak heights taken from the DPV and produced a linear regression curve which can be seen in the inset line curve in Figure 3D. From this curve, we have a linear response in serum between the concentrations of 100 nM and 2 μM and a

sensitivity of 7.9 μA μM^{-1} cm^{-2} with an R^2 value of 0.99 and a clear detection limit of 50 nM. As expected, the sensitivity and LOD decrease for the GC-PSS sensor in the presence of serum. However, these results still show that not only is our sensor viable in serum but is highly effective within the physiological range of serotonin serum concentration ranges (0.27−1.5 μM).

4. CONCLUSIONS

Here we have developed and demonstrated a highly sensitive and selective serotonin sensor using an electrodeposited PSS thin film. The sensor can be fabricated using a simple, inexpensive one-step electrodeposition onto GC. The deposition of the semiselective polymeric matrix can be performed in less than 2 min and used immediately without further modification. Similarly, to other serotonin sensors that leverage polymeric matrices, the GC-PSS sensor should be more inert to biodegradation, changes in temperature, pH, and denaturant concentrations, compared to traditional biorecognition elements. The uniqueness of this sensor is that in contrast to other reported serotonin sensors, a significant change in the electrostatic state and thus the redox potential of serotonin is observed when the PSS capture element is present, resulting in superlative observed sensor properties. Notably, the sensor presented here has an excellent sensitivity of 179 μA μM^{-1} cm^{-2}; the linear detection range based on experimental data was demonstrated to be 0.01−1 μM; this range is a 36× enhancement of the LOD compared to the unmodified GC electrode surface and a 3× enhancement compared to GC-PEDOT/PSS. The sensor was also shown to be highly effective in 100% human serum displaying a linear range between 100 nM and 2 μM with a sensitivity of 7.9 μA μM^{-1} cm^{-2} and a detection limit of 50 nM. Therefore, the reported serotonin sensor provides a robust sensor for near real-time analysis of serotonin demonstrated both at physiological concentrations and in physiological fluids that can be deployed in emerging sensor platforms. Finally, this paper demonstrates the benefit and utility of rational design and selection of polymeric matrices to detect key analytes of interest.

■ ASSOCIATED CONTENT

Ⓢ Supporting Information

The Supporting Information is available free of charge at https://pubs.acs.org/doi/10.1021/acsomega.4c01169.

> DPV curves of GC and PEDOT/PSS sensors; DPV results of GC-PSS sensors at various electrodeposition times in serotonin and their % peak current change analysis; Linear regression curves of GC-PSS, GC, and PEDOT/PSS sensors; peak potential shift of GC-PSS sensor in varying Human serum concentrations; table to contaminants concentrations; discussion and DPV analysis of equilibrium time analysis; table of added concentrations for calibration curve validation (PDF)

■ AUTHOR INFORMATION

Corresponding Author

Steve S. Kim − *Human Effectiveness Directorate, 711th Human Performance Wing, Air Force Research Laboratory, Wright-Patterson AFB, Ohio 45433, United States;* ⓞ orcid.org/0000-0002-9519-077X; Phone: 937-938-3797; Email: steve.kim.13@us.af.mil

Authors

Victoria E. Coyle − *Human Effectiveness Directorate, 711th Human Performance Wing, Air Force Research Laboratory, Wright-Patterson AFB, Ohio 45433, United States; UES Inc., Dayton, Ohio 45432, United States;* ⓞ orcid.org/0009-0001-4365-0180

Michael C. Brothers − *Human Effectiveness Directorate, 711th Human Performance Wing, Air Force Research Laboratory, Wright-Patterson AFB, Ohio 45433, United States; UES Inc., Dayton, Ohio 45432, United States;* ⓞ orcid.org/0000-0002-8239-2399

Sarah McDonald − *Human Effectiveness Directorate, 711th Human Performance Wing, Air Force Research Laboratory, Wright-Patterson AFB, Ohio 45433, United States; UES Inc., Dayton, Ohio 45432, United States*

Complete contact information is available at:
https://pubs.acs.org/10.1021/acsomega.4c01169

Notes

The authors declare no competing financial interest.

■ ACKNOWLEDGMENTS

■ REFERENCES

(1) Leu, F.; Ko, C.; You, I.; Choo, K. K. R.; Ho, C. L. A smartphone-based wearable sensors for monitoring real-time physiological data. *Comput. Electr. Eng.* **2018**, *65*, 376−392.

(2) Apiletti, D.; Baralis, E.; Bruno, G.; Cerquitelli, T. Real-time analysis of physiological data to support medical applications. *IEEE Trans. Inf. Technol. Biomed.* **2009**, *13* (3), 313−321.

(3) Ates, H. C.; Nguyen, P. Q.; Gonzalez-Macia, L.; Morales-Narváez, E.; Güder, F.; Collins, J. J.; Dincer, C. End-to-end design of wearable sensors. *Nat. Rev. Mater.* **2022**, *7* (11), 887−907.

(4) Banerjee, S.; McCracken, S.; Hossain, M. F.; Slaughter, G. Electrochemical detection of neurotransmitters. *Biosensors* **2020**, *10* (8), 101−109.

(5) Tavakolian-Ardakani, Z.; Hosu, O.; Cristea, C.; Mazloum-Ardakani, M.; Marrazza, G. Latest trends in electrochemical sensors for neurotransmitters: A review. *Sensors* **2019**, *19* (9), 2037−2067.

(6) Borgmann, S.; Hartwich, G.; Schulte, A.; Schuhmann, W. Amperometric enzyme sensors based on direct and mediated electron transfer. In *Perspectives in Bioanalysis*; Elsevier, 2005; Vol. 1, pp 599−655.

(7) Wang, H.; Yang, T.; Wu, J.; Chen, D.; Wang, W. Unveiling the Mystery of SUMO-activating enzyme subunit 1: A Groundbreaking Biomarker in the Early Detection and Advancement of Hepatocellular Carcinoma. *Transplant. Proc.* **2023**, 945−951.

(8) Chiu, W. K.; Towheed, A.; Palladino, M. J. Genetically encoded redox sensors. *Methods Enzymol.* **2014**, *542*, 263−287.

(9) Zhou, L.; Liu, Y.; Sun, H.; Li, H.; Zhang, Z.; Hao, P. Usefulness of enzyme-free and enzyme-resistant detection of complement component 5 to evaluate acute myocardial infarction. *Sens. Actuators, B* **2022**, *369*, 132315.

(10) Jiang, M.; Wang, C.; Zhang, X.; Cai, C.; Ma, Z.; Chen, J.; Xie, T.; Huang, X.; Chen, D. A cellular nitric oxide sensor based on porous hollow fiber with flow-through configuration. *Biosens. Bioelectron.* **2021**, *191*, 113442.

(11) Özel, R. E.; Hayat, A.; Andreescu, S. Recent developments in electrochemical sensors for the detection of neurotransmitters for applications in biomedicine. *Anal. Lett.* **2015**, *48* (7), 1044−1069.

(12) Su, Y.; Bian, S.; Sawan, M. Real-time in vivo detection techniques for neurotransmitters: A review. *Analyst* **2020**, *145* (19), 6193−6210.

(13) Yao, H.; Li, S.; Tang, Y.; Chen, Y.; Chen, Y.; Lin, X. Selective oxidation of serotonin and norepinephrine over eriochrome cyanine R film modified glassy carbon electrode. *Electrochim. Acta* **2009**, *54* (20), 4607−4612.

(14) Huang, H.; Chen, Z.; Yan, X. Simultaneous determination of serotonin and creatinine in urine by combining two ultrasound-assisted emulsification microextractions with on-column stacking in capillary electrophoresis. *J. Sep. Sci.* **2012**, *35* (3), 436−444.

(15) Lindström, M.; Tohmola, N.; Renkonen, R.; Hämäläinen, E.; Schalin-Jäntti, C.; Itkonen, O. Comparison of serum serotonin and serum 5-HIAA LC-MS/MS assays in the diagnosis of serotonin producing neuroendocrine neoplasms: A pilot study. *Clin. Chim. Acta* **2018**, *482*, 78−83.

(16) Rognum, I. J.; Tran, H.; Haas, E. A.; Hyland, K.; Paterson, D. S.; Haynes, R. L.; Broadbelt, K. G.; Harty, B. J.; Mena, O.; Krous, H. F.; et al. Serotonin metabolites in the cerebrospinal fluid in sudden infant death syndrome. *J. Neuropathol. Exp. Neurol.* **2014**, *73* (2), 115−122.

(17) Kucherenko, I.; Topolnikova, Y. V.; Soldatkin, O. Advances in the biosensors for lactate and pyruvate detection for medical applications: a review. *TrAC, Trends Anal. Chem.* **2019**, *110*, 160−172.

(18) Yoo, E.-H.; Lee, S.-Y. Glucose biosensors: an overview of use in clinical practice. *Sensors* **2010**, *10* (5), 4558−4576.

(19) Bai, L.; Wen, D.; Yin, J.; Deng, L.; Zhu, C.; Dong, S. Carbon nanotubes-ionic liquid nanocomposites sensing platform for NADH oxidation and oxygen, glucose detection in blood. *Talanta* **2012**, *91*, 110−115.

(20) Senel, M.; Dervisevic, E.; Alhassen, S.; Dervisevic, M.; Alachkar, A.; Cadarso, V. J.; Voelcker, N. H. Microfluidic electrochemical sensor for cerebrospinal fluid and blood dopamine detection in a mouse model of Parkinson's disease. *Anal. Chem.* **2020**, *92* (18), 12347−12355.

(21) Chen, J.-C.; Chung, H.-H.; Hsu, C.-T.; Tsai, D.-M.; Kumar, A.; Zen, J.-M. A disposable single-use electrochemical sensor for the detection of uric acid in human whole blood. *Sens. Actuators, B* **2005**, *110* (2), 364−369.

(22) Hashemi, S. A.; Mousavi, S. M.; Bahrani, S.; Ramakrishna, S.; Babapoor, A.; Chiang, W.-H. Coupled graphene oxide with hybrid metallic nanoparticles as potential electrochemical biosensors for precise detection of ascorbic acid within blood. *Anal. Chim. Acta* **2020**, *1107*, 183−192.

(23) Dong, S.; Bi, Q.; Qiao, C.; Sun, Y.; Zhang, X.; Lu, X.; Zhao, L. Electrochemical sensor for discrimination tyrosine enantiomers using graphene quantum dots and β-cyclodextrins composites. *Talanta* **2017**, *173*, 94−100.

(24) Goyal, R. N.; Gupta, V. K.; Oyama, M.; Bachheti, N. Gold nanoparticles modified indium tin oxide electrode for the simultaneous determination of dopamine and serotonin: application in pharmaceutical formulations and biological fluids. *Talanta* **2007**, *72* (3), 976−983.

(25) Thanh, T. D.; Balamurugan, J.; Hien, H. V.; Kim, N. H.; Lee, J. H. A novel sensitive sensor for serotonin based on high-quality of AuAg nanoalloy encapsulated graphene electrocatalyst. *Biosens. Bioelectron.* **2017**, *96*, 186−193.

(26) Zhou, J.; Sheng, M.; Jiang, X.; Wu, G.; Gao, F. Simultaneous determination of dopamine, serotonin and ascorbic acid at a glassy carbon electrode modified with carbon-spheres. *Sensors* **2013**, *13* (10), 14029−14040.

(27) Jiang, M.; Zhu, L.; Liu, Y.; Li, J.; Diao, Y.; Wang, C.; Guo, X.; Chen, D. Facile fabrication of laser induced versatile graphene-metal nanoparticles electrodes for the detection of hazardous molecules. *Talanta* **2023**, *257*, 124368.

(28) Al-Graiti, W.; Foroughi, J.; Liu, Y.; Chen, J. Hybrid graphene/conducting polymer strip sensors for sensitive and selective electrochemical detection of serotonin. *ACS Omega* **2019**, *4* (26), 22169−22177.

(29) Song, M.-J.; Kim, S.; Ki Min, N.; Jin, J.-H. Electrochemical serotonin monitoring of poly (ethylenedioxythiophene): poly (sodium 4-styrenesulfonate)-modified fluorine-doped tin oxide by predeposition of self-assembled 4-pyridylporphyrin. *Biosens. Bioelectron.* **2014**, *52*, 411−416.

(30) Tertiş, M.; Cernat, A.; Lacatiş, D.; Florea, A.; Bogdan, D.; Suciu, M.; Săndulescu, R.; Cristea, C. Highly selective electrochemical detection of serotonin on polypyrrole and gold nanoparticles-based 3D architecture. *Electrochem. commun.* **2017**, *75*, 43−47.

(31) Uwaya, G. E.; Fayemi, O. E. Electrochemical detection of serotonin in banana at green mediated PPy/Fe3O4NPs nanocomposites modified electrodes. *Sens. Bio-Sens. Res.* **2020**, *28*, 100338−100349.

(32) Adhikari, A.; Nath, J.; Rana, D.; De, S.; Chakraborty, M.; Kar, P.; Chakraborty, A. K.; Chattopadhyay, D. Electrochemical sensing of serotonin by silver decorated polypyrrole nanoribbon based electrode synthesized by sodium cholate as soft template. *Mater. Today Commun.* **2022**, *31*, 103361−103369.

(33) Babaei, A.; Taheri, A. R. Nafion/Ni (OH) 2 nanoparticles-carbon nanotube composite modified glassy carbon electrode as a sensor for simultaneous determination of dopamine and serotonin in the presence of ascorbic acid. *Sens. Actuators, B* **2013**, *176*, 543−551.

(34) Selvaraju, T.; Ramaraj, R. Electrochemically deposited nanostructured platinum on Nafion coated electrode for sensor applications. *J. Electroanal. Chem.* **2005**, *585* (2), 290−300.

(35) Demuru, S.; Deligianni, H. Surface PEDOT: nafion coatings for enhanced dopamine, serotonin and adenosine sensing. *J. Electrochem. Soc.* **2017**, *164* (14), G129−G138.

(36) Rubinstein, I.; Bard, A. J. Polymer films on electrodes. 5. Electrochemistry and chemiluminescence at Nafion-coated electrodes. *J. Am. Chem. Soc.* **1981**, *103* (17), 5007−5013.

(37) Moon, J.-M.; Thapliyal, N.; Hussain, K. K.; Goyal, R. N.; Shim, Y.-B. Conducting polymer-based electrochemical biosensors for neurotransmitters: A review. *Biosens. Bioelectron.* **2018**, *102*, 540−552.

(38) Xu, G.; Li, B.; Cui, X. T.; Ling, L.; Luo, X. Electrodeposited conducting polymer PEDOT doped with pure carbon nanotubes for the detection of dopamine in the presence of ascorbic acid. *Sens. Actuators, B* **2013**, *188*, 405−410.

(39) Wang, M.-H.; Ji, B.-W.; Gu, X.-W.; Tian, H.-C.; Kang, X.-Y.; Yang, B.; Wang, X.-L.; Chen, X.; Li, C.-Y.; Liu, J.-Q. Direct electrodeposition of Graphene enhanced conductive polymer on microelectrode for biosensing application. *Biosens. Bioelectron.* **2018**, *99*, 99−107.

(40) Binninger, T.; Fabbri, E.; Kötz, R.; Schmidt, T. J. Determination of the electrochemically active surface area of metal-oxide supported platinum catalyst. *J. Electrochem. Soc.* **2014**, *161* (3), H121−H128.

(41) Coyle, V. E.; Kandjani, A. E.; Sabri, Y. M.; Bhargava, S. K. Au Nanospikes as a Non-enzymatic Glucose Sensor: Exploring Morphological Changes with the Elaborated Chronoamperometric Method. *Electroanalysis* **2017**, *29* (1), 294−304.

(42) Nath, A. K.; Ghatak, A.; Dey, A.; Dey, S. G. Intermediates involved in serotonin oxidation catalyzed by Cu bound Aβ peptides. *Chem. Sci.* **2021**, *12* (5), 1924−1929.

(43) Coughlin, J. E.; Reisch, A.; Markarian, M. Z.; Schlenoff, J. B. Sulfonation of polystyrene: Toward the "ideal" polyelectrolyte. *J. Polym. Sci., Part A: Polym. Chem.* **2013**, *51* (11), 2416−2424.

(44) Sadanandhan, N. K.; Cheriyathuchenaaramvalli, M.; Devaki, S. J.; Ravindranatha Menon, A. PEDOT-reduced graphene oxide-silver hybrid nanocomposite modified transducer for the detection of serotonin. *J. Electroanal. Chem.* **2017**, *794*, 244−253.

(45) Sun, D.; Li, H.; Li, M.; Li, C.; Dai, H.; Sun, D.; Yang, B. Electrodeposition synthesis of a NiO/CNT/PEDOT composite for simultaneous detection of dopamine, serotonin, and tryptophan. *Sens. Actuators, B* **2018**, *259*, 433−442.

(46) Li, Y.-T.; Tang, L.-N.; Ning, Y.; Shu, Q.; Liang, F.-X.; Wang, H.; Zhang, G.-J. In vivo monitoring of serotonin by nanomaterial functionalized acupuncture needle. *Sci. Rep.* **2016**, *6* (1), 28018.

(47) Atta, N. F.; Galal, A.; Ahmed, R. A. Simultaneous determination of catecholamines and serotonin on poly (3, 4-ethylene dioxythiophene) modified Pt electrode in presence of sodium dodecyl sulfate. *J. Electrochem. Soc.* **2011**, *158* (4), F52−F60.